# Bonding in Elongated Dihydrogen Complexes. Theoretical Analysis of the Electron Density in [$ML_n(H\cdots H)$] Species

Feliu Maseras,*[,†,‡] Agustí Lledós,*[,†] Miquel Costas,[§] and Josep M. Poblet[§]

*Unitat de Química Física, Departament de Química, Universitat Autònoma de Barcelona, 08193 Bellaterra, Barcelona, Catalonia, Spain, and Departament de Química, Universitat Rovira i Virgili, 43005 Tarragona, Catalonia, Spain*

*Received December 5, 1995*[⊗]

The geometry of a series of four [$ML_n$"$H_2$"] complexes ($W(H_2)(CO)_3(PR_3)_2$, $IrH(H\cdots H)Cl_2(PR_3)_2$, $[Os(H\cdots H)(NH_2(CH_2)_2NH_2)_2(RCO_2)]^+$, and $OsH_4(PR_3)_3$) spanning a large range of H−H values is optimized at the B3LYP computational level, yielding satisfactory agreement with available neutron-diffraction data. The electron density resulting from these theoretical calculations is analyzed afterward within the "atoms in molecules" formalism, resulting in a positive assignment of the complexes $W(H_2)(CO)_3(PR_3)_2$ and $IrH(H\cdots H)Cl_2(PR_3)_2$ as dihydrogen complexes and of the complexes $[Os(H\cdots H)(NH_2(CH_2)_2NH_2)_2(RCO_2)]^+$ and $OsH_4(PR_3)_3$ as dihydride complexes.



## Introduction

Characterization of transition metal dihydrogen complexes has probably been one of the most exciting developments in coordination chemistry in the last decade.[1] Their discovery has reshaped the view on the way $\sigma$ bonds interact with metal atoms. Only 15 years ago, it was considered that coordination of a hydrogen molecule to a metal complex leads necessarily to the breaking of the H−H bond and the formation of two M−H bonds, resulting in a dihydride complex with the bonding structure shown in the left-hand side of Chart 1. Nowadays, the existence of species where the hydrogen bond is not broken, namely dihydrogen complexes, is fully accepted. Dihydrogen complexes may in principle be represented by any of the bonding structures in the right-hand side of Chart 1. Bonding in these species is already well understood.[2] There are an ever-growing number of reports concerning them in the literature, and the effect of their presence in a number of different processes is starting to be appreciated. Moreover, all developments in their chemistry have a direct impact on the even wider field of $\sigma$ bond activation.[3]

Nevertheless, there remain dark areas in the characterization itself of dihydrogen complexes. The drawings in Chart 1 imply that the reaction $ML_n + H_2 \rightarrow ML_n$"$H_2$" can give rise to either a dihydride complex or to a dihydrogen complex but that there is no other possible product in between. That is, all complexes with this stoichiometry should belong to one of the two classes. There is indeed a range of H−H distances considered "normal" for dihydrogen complexes (shorter than 0.85 Å) and another range considered "normal" for dihydride complexes (larger than 1.50 Å), and neutron diffraction experiments[4−6] have allowed the unequivocal assignment of a number of species[4−6] according to this criterion. However, even within the still scarce number of neutron diffraction studies available on this type of species,[4−9] there are some examples which lie outside the "common sense" ranges just mentioned.[7−9] These are the so-called elongated dihydrogen complexes, which

**Chart 1**

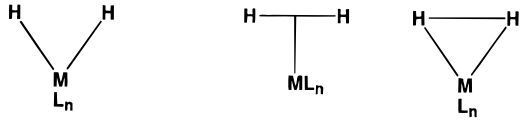


Dihydride Complex | Dihydrogen Complex

† Universitat Autònoma de Barcelona.
‡ Current address: Laboratoire de Structure et Dynamique des Systèmes Moléculaires et Solides, UMR 5636, Université de Montpellier II, 34095 Montpellier Cedex 5, France.
§ Universitat Rovira i Virgili.
⊗ Abstract published in *Advance ACS Abstracts,* May 15, 1996.

(1) (a) Kubas, G. J. *Acc. Chem. Res.* **1988**, *21*, 120−128. (b) Crabtree, R. H. *Acc. Chem. Res.* **1990**, *23*, 95−101. (c) Jessop, P. J.; Morris, R. H. *Coord. Chem. Rev.* **1992**, *121*, 155−284. (d) Heinekey, D. M.; Oldham, W. J., Jr. *Chem. Rev.* **1993**, *93*, 913−926.

(2) (a) Burdett, J. K.; Eisenstein, O.; Jackson, S. A. In *Transition Metal Hydrides*; Dedieu, A., Ed.; VCH: Weinheim, Germany, 1991; pp 149−184. (b) Lin, Z.; Hall, M. B. *Coord. Chem. Rev.* **1994**, *135*, 845−879.

(3) (a) Crabtree, R. H.; Hamilton, D. G. *Adv. Organomet. Chem.* **1988**, *28*, 299−338. (b) Crabtree, R. H. *Angew. Chem., Int. Ed. Engl.* **1993**, *32*, 789−805.

(4) (a) Ricci, J. S.; Koetzle, T. F.; Bautista, M. T.; Hofstede, T. M.; Morris, R. H.; Sawyer, J. F. *J. Am. Chem. Soc.* **1989**, *111*, 8823−8827. (b) Van Der Sluys, L. S.; Eckert, J.; Eisenstein, O.; Hall, J. H.; Huffman, J. C.; Jackson, S. A.; Koetzle, T. F.; Kubas, G. J.; Vergamini, P. J.; Caulton, K. G. *J. Am. Chem. Soc.* **1990**, *112*, 4831−4841. (c) Kubas, G. J.; Burns, C. J.; Eckert, J.; Johnson, W. W.; Larson, A. C.; Vergamini, P. J.; Unkefer, C. J.; Khalsa, G. R. K.; Jackson, S. A.; Eisenstein, O. *J. Am. Chem. Soc.* **1993**, *115*, 569−581.

(5) (a) Kubas, G. J.; Ryan, R. R.; Swanson, B. I.; Vergamini, P. J.; Wasserman, H. J. *J. Am. Chem. Soc.* **1984**, *100*, 451−452. (b) Vergamini, P. J.; Wasserman, H. J.; Koetzle, T. F.; Kubas, G. J. Unpublished work cited in footnote 9 of: Kubas, G. J.; Unkefer, C. J.; Swanson, B. J.; Fukushima, E. *J. Am. Chem. Soc.* **1986**, *108*, 7000−7009.

(6) Hart, D. W.; Bau, R.; Koetzle, T. F. *J. Am. Chem. Soc.* **1977**, *99*, 7557−7564.

(7) (a) Bramner, L.; Howard, J. A. K.; Johnson, O.; Koetzle, T. F.; Spencer, J. L.; Stringer, A. M. *J. Chem. Soc., Chem. Commun.* **1991**, 241−243. (b) Klooster, W. T.; Koetzle, T.; Jia, G.; Fong, T. P.; Morris, R. H.; Albinati, A. *J. Am. Chem. Soc.* **1994**, *116*, 7677−7681.

(8) Albinati, A.; Bakhmutov, V. I.; Caulton, K. G.; Clot, E.; Eckert, J.; Eisenstein, O.; Gusev, D. G.; Grushin, V. V.; Hauger, B. E.; Klooster, W. T.; Koetzle, T. F.; McMullan, R. K.; O'Loughlin, T. J.; Pélissier, M.; Ricci, J. S.; Sigalas, M. P.; Vymenits, A. B. *J. Am. Chem. Soc.* **1993**, *115*, 7300−7312.

(9) Hasegawa, T.; Li, Z.; Parkin, S.; Hope, H.; McMullan, R. K.; Koetzle, T. F.; Taube, H. *J. Am. Chem. Soc.* **1994**, *116*, 4352−4356.

S0276-7333(95)00936-8 CCC: $12.00 

could be loosely defined as complexes showing a H−H distance too long for a dihydrogen but too short for a dihydride.

The problem of assignment of elongated dihydrogen complexes as true dihydrogen complexes or as true dihydride complexes is intrinsically unsolvable by the neutron diffraction technique, because this method can only locate atomic nuclei but not chemical bonds. Remarkably enough, this problem can be solved in principle by theoretical chemistry through the use of the "atoms in molecules" theory developed by Bader and coworkers.[10,11] This is an analysis scheme that allows, given an electron density, to locate the bonds between atoms. Certainly, the presence of a chemical bond is mathematically characterized in an univocal way by the presence of a bond critical point, which is defined as a zero-gradient point having one positive and two negative eigenvalues in the 3-dimensional space representation of the charge density function.

This paper presents the application of this analysis scheme to four different complexes spanning the whole range of possible cases. These are $W(H_2)(CO)_3(P^iPr_3)_2$ (**1a**),[5] $Ir(H\cdots H)(H)Cl_2(P^iPr_3)_2$ (**2a**),[8] $[Os(H\cdots H)(NH_2(CH_2)_2NH_2)_2(CH_3CO_2)]^+$ (**3a**),[9] and $OsH_4(PMe_2Ph)_3$ (**4a**).[6] There are neutron diffraction data for each of them, and the H−H distances are respectively 0.82, 1.11, 1.34, and 1.84 Å. That is, there are one dihydrogen complex (**1a**), one dihydride complex (**4a**), and two species that may be described as elongated dihydrogen complexes (**2a** and **3a**), although having quite different H−H distances.

## Computational Details

All calculations were carried out with the Gaussian 92/DFT[12] and Gaussian 94[13] series of programs. The density functional theory[14] was applied, with the nonlocal functions labeled as B3LYP.[13] This function consists of Becke's three-parameter hybrid method for the exchange part[15] and the Lee−Yang−Parr expression for the correlation part.[16] All geometry optimizations were complete within the symmetry restrictions indicated below for each complex, with the only exception of dihedral angles involving rotation around M−P bonds. The topological properties of the electron density were calculated with a version of the AIMPAC package.[17]

An effective core potential operator was used to represent the 60 innermost electrons (up to the 4d shell) of the transition metal atoms.[18] For these metal atoms, the basis set was that associated with the pseudopotential,[18] with a standard valence double-ζ contraction.[12,13] The basis set for the hydrogen atoms directly attached to the metal was double-ζ, supplemented with a polarization p shell.[19,20] A valence double-ζ basis set was used for most of the other H atoms, as well as for C, N, and O atoms,[19] with the only exception of the $-(CH_2)_2-$ groups of the chelating ligand in complex **3b**, which were described with a minimal basis.[21] Finally, the P and Cl atoms were described with a double-ζ plus polarization basis set.[22]

**Table 1. B3LYP-Optimized Values of the H−H and M−H Distances for Model Complexes 1b−4b, Compared with Available Neutron Diffraction Data for Complexes 1a−4a[a]**

| | | 1 | 2 | 3 | 4 |
|---|---|---|---|---|---|
| H−H | B3LYP | 0.818 | 0.984 | 1.428 | 1.861 |
| | neutron | 0.82 | 1.11 | 1.34 | 1.84 |
| M−H | B3LYP | 1.934 | 1.651 | 1.606 | 1.641 |
| | neutron | 1.95 | 1.54 | 1.60 | 1.65 |

[a] All distances are in Å.

## Geometry Optimization of Model Complexes

We have carried out geometry optimization calculations on each of the four model complexes $W"H_2"(CO)_3(PH_3)_2$ (**1b**), $Ir"H_3"Cl_2(PH_3)_2$ (**2b**), $[Os"H_2"(NH_2(CH_2)_2NH_2)_2(HCO_2)]^+$ (**3b**), and $Os"H_4"(PH_3)_3$ (**4b**). Their relationship with the experimental complexes **1a**−**4a** is straightforward, following the usual practice in ab initio calculations of replacing the bulky $\sigma$-bonded substituents far from the metal center by hydrogen atoms.[23] The goal of the geometry optimization in this work is to check the accuracy of the computational level. An analysis of the electron density in single point calculations on the experimental geometries would be much more arguable, especially because elongated dihydrogen complexes have proved to be an elusive target for computational chemistry.[2b,8]

After a number of technical tests, we decided to use a DFT-based[14] B3LYP methodology,[15,16] which succeeded in providing much more satisfactory results than the more widespread RHF-based MP2 approach[24] in the geometry optimization of these complexes (*vide infra*). The more technical aspects about the calculations can be found in the Computational Details section.

Table 1 collects the experimental and computed values of the two most relevant parameters for each of the four complexes, the H−H and M−H distances. Although agreement between computation and experiment is far from perfect (discrepancies of up to 0.13 Å in H−H distances and up to 0.11 Å in M−H distances), the experimental trend in H−H distances is without any doubt properly reproduced by the theoretical calculations. This is the interpretation we extract from the correspondence between the experimental series of values of 0.84, 1.11, 1.34, and 1.84 Å and the theoretical



(10) Bader, R. F. W. *Atoms in Molecules. A Quantum Theory*; Oxford University Press: Oxford, U.K., 1994.
(11) (a) Bader, R. F. W.; Anderson, S. G.; Duke, A. J. *J. Am. Chem. Soc.* **1979**, *101*, 1389−1395. (b) Bader, R. F. W. *Chem. Rev.* **1991**, *91*, 893−928.
(12) Frisch, M. J.; Trucks, G. W.; Schlegel, H. B.; Gill, P. M. W.; Johnson, B. G.; Wong, M. W.; Foresman, J. B.; Robb, M. A.; Head-Gordon, M.; Replogle, E. S.; Gomperts, R.; Andres, J. L.; Raghavachari, K.; Binkley, J. S.; Gonzalez, C.; Martin, R. L.; Fox, D. J.; Defrees, D. J.; Baker, J.; Stewart, J. J. P.; Pople, J. A. *Gaussian 92/DFT*; Gaussian, Inc.: Pittsburgh, PA, 1993.
(13) Frisch, M. J.; Trucks, G. W.; Schlegel, H. B.; Gill, P. M. W.; Johnson, B. G.; Robb, M. A.; Cheeseman, J. R.; Keith, T.; Petersson, G. A.; Montgomery, J. A.; Raghavachari, K.; Al-Laham, M. A.; Zakrzewski, V. G.; Ortiz, J. V.; Foresman, J. B.; Peng, C. Y.; Ayala, P. Y.; Chen, W.; Wong, M. W.; Andres, J. L.; Replogle, E. S.; Gomperts, R.; Martin, R. L.; Fox, D. J.; Binkley, J. S.; Defrees, D. J.; Baker, J.; Stewart, J. P.; Head-Gordon, M.; Gonzalez, C.; Pople, J. A. *Gaussian 94*; Gaussian, Inc.: Pittsburgh, PA, 1995.
(14) (a) Parr, R. G.; Yang, W. *Density-Functional Theory of Atoms and Molecules*; Oxford University Press: Oxford, U.K., 1989. (b) Ziegler, T. *Chem. Rev.* **1991**, *91*, 651−668.
(15) Becke, A. D. *J. Chem. Phys.* **1993**, *98*, 5648−5652.
(16) Lee, C.; Yang, W.; Parr, R. G. *Phys. Rev. B* **1988**, *37*, 785−789.
(17) Biegler-König, F. W.; Bader, R. F. W.; Tang, T. H. *J. Comput. Chem.* **1982**, *3*, 317−328.
(18) Hay, P. J.; Wadt, W. R. *J. Chem. Phys.* **1985**, *82*, 299−310.
(19) Hehre, W. J.; Ditchfield, R.; Pople, J. A. *J. Chem. Phys.* **1972**, *56*, 2257−2261.
(20) Hariharan, P. C.; Pople, J. A. *Theor. Chim. Acta* **1973**, *28*, 213.
(21) Hehre, W. J.; Stewart, R. F.; Pople, J. A. *J. Chem. Phys.* **1969**, *51*, 2657−2667.
(22) Francl, M. M.; Pietro, W. J.; Hehre, W. J.; Binkley, J. S.; Gordon, M. S.; DeFrees, D. J.; Pople, J. A. *J. Chem. Phys.* **1982**, *77*, 3654−3665.
(23) (a) Veillard, A. *Chem. Rev.* **1991**, *91*, 743−766. (b) Koga, N.; Morokuma, K. *Chem. Rev.* **1991**, *91*, 823−842.
(24) Møller, C.; Plesset, M. S. *Phys. Rev.* **1934**, *46*, 618.

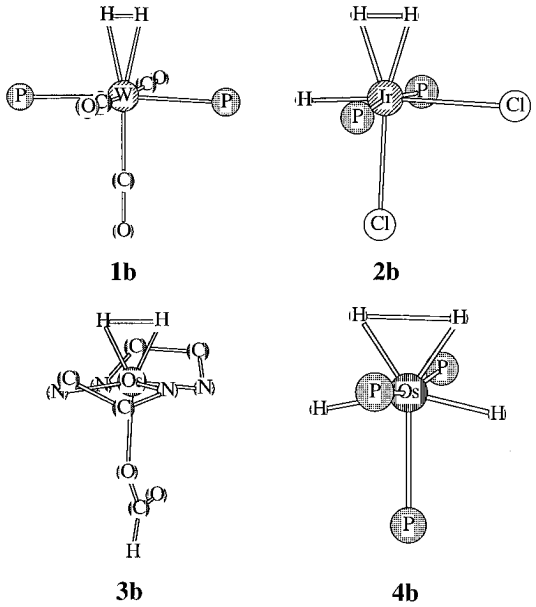


**Figure 1.** B3LYP-optimized geometries of model complexes **1b**, **2b**, **3b**, and **4b**. Most of hydrogen atoms not directly attached to the metal atoms are omitted for clarity.

series of 0.818, 0.984, 1.428, and 1.861 Å. There is certainly not such a trend in M−H distances, neither in experiment nor in computation, but it could hardly be expected, since the metal and ligand environments are different for each complex.

Figure 1 presents the optimized geometry for complexes **1b**−**4b**. The M−$H_2$ subunit has been represented as a bonded triangle in all cases to avoid any prejudgement on the bonding scheme, which will be discussed in depth in the next section. In what remains of this section, we will briefly discuss the particular geometrical features of each one of the complexes. The full set of Cartesian coordinates, as well as the total energies, are provided as Supporting Information.

Complex **1a** is the first dihydrogen complex that was ever characterized[5] and has consequently received a remarkable amount of attention from both experimentalists[1] and theoreticians.[2,25,26] Neutron diffraction data indicate an octahedral coordination, with the dihydrogen ligand, oriented parallel to the P−W−P direction, occupying one of the sites. Our $C_s$ geometry optimization of **1b** yielded an almost perfect octahedron, the largest deviation being smaller than 2°. The geometry of the W−$H_2$ fragment is computed with high accuracy (Table 1), the discrepancies with experiment being inferior to 0.02 Å. Not surprisingly, these results are significantly better than those of the very first ab initio study on dihydrogen complexes,[26] which was carried out on this same complex, but with a poorer RHF description. Our computed values for both W−P (2.469 Å) and W−C (1.977−2.025 Å) distances are also close to X-ray values for a related species (2.458−2.493 Å for W−P, 1.899−1.998 Å for W−C).[27]

Complex **2a**, with its H−H distance of 1.11 Å,[8] was the first species shown by neutron diffraction to have an H−H distance larger than 0.9 Å and smaller than 1.30 Å. As a result, it received the attention of theoretical chemists.[2,8] However, the MP2 methodology, very efficient in related species,[28−30] was shown to be unable to locate this species as a local minimum in the potential hypersurface (optimized H−H distance of 1.4 Å).[8] We found similar results in our own tests with the MP2 method on **2b**, and we actually used this particular complex as the test for the methodology. Our $C_s$-optimized B3LYP geometry (Table 1) shows a much closer resemblance to experiment than that obtained from MP2. We are therefore confident that our calculation is able to reproduce, at least at a qualitative level, the nature of bonding in complex **2**. Apart from the particularities of the Ir−$H_2$ bonding, other geometrical features of complex **2** are properly described. If one considers the dihydrogen to be a single ligand, this complex is an octahedral $ML_6$ species, with the two atoms of the dihydrogen unit coplanar with the metal, the hydride, and the two chloride ligands. A remarkable distortion from the regular octahedron corresponds to the two cis ligands coplanar with the dihydrogen, and it is reproduced in the calculation (H−Ir−Cl angle: experiment, 170.2°; calculation, 174.9°). The difference in the two Ir−Cl distances, being longer that trans to hydride (experiment, 2.50 Å; theory, 2.542 Å) than that trans to dihydrogen (experiment 2.45 Å; theory, 2.421 Å), is also reproduced.

Complex **3a**, though having a quite longer H−H distance (1.36 Å), has also been labeled as $\eta^2$-$H_2$ based on its value for $J_{H-D}$ of 9.0 Hz.[9] If it were to be considered as a true dihydrogen complex, it would also have an octahedral geometry, with the dihydrogen unit trans to the acetate ligand. In this case, the dihydrogen unit does not lie parallel to any of the cis N−Os−N directions but rather in one of the bisectors. Alternatively, if one viewed the complex as a 7-coordinate dihydride species, it would be a capped trigonal prism,[31] with the acetate ligand in the capping position. These geometrical features are well reproduced in our $C_1$ B3LYP geometry optimization of **3b**, as well as bonding in the Os−$H_2$ fragment (Table 1). Our results are in good agreement with those obtained in an MP2 study addressed to the same complex **3a** but with a different $[Os(H_2)(NH_3)_4(OAc)]^+$ modelization.[32] In that case, the optimized values for H−H and Os−H were 1.39 and 1.58 Å, respectively. Our computed values for the Os−N (2.167−2.188 Å) and Os−O (2.173 Å) distances are also reasonably close to the experimental values (2.110−2.143 Å for Os−N and 2.141 Å for Os−O).[9]

Complex **4a** has been chosen as example of a polyhydride complex with nonbonded cis hydride ligands.[6] Its coordination polyhedron is a pentagonal bipyramid, with two phosphine ligands occupying the axial sites. The four hydride ligands give rise to three contiguous H−H contacts. The three associated H−H distances, always larger than 1.80 Å, are quite similar. We have chosen



(25) Jean, Y.; Eisenstein, O.; Volatron, F.; Maouche, B.; Sefta, F. *J. Am. Chem. Soc.* **1986**, *108*, 6587−6592.
(26) Hay, P. J. *J. Am. Chem. Soc.* **1987**, *109*, 705−710.
(27) Wasserman, H. J.; Kubas, G. J.; Ryan, R. R. *J. Am. Chem. Soc.* **1986**, *108*, 2294−2301.
(28) Lin, Z.; Hall, M. B. *J. Am. Chem. Soc.* **1992**, *114*, 2928−2932.
(29) Maseras, F.; Koga, N.; Morokuma, K. *J. Am. Chem. Soc.* **1993**, *115*, 8313−8320.
(30) Maseras, F.; Li, X.-K.; Koga, N.; Morokuma, K. *J. Am. Chem. Soc.* **1993**, *115*, 10974−10980.
(31) (a) Drew, M. G. B. *Prog. Inorg. Chem.* **1977**, *23*, 67−210. (b) Kepert, D. L. *Inorganic Stereochemistry*; Springer-Verlag: Berlin, 1982.
(32) (a) Craw, J. S.; Backsay, G. B.; Hush, N. S. *Inorg. Chem.* **1993**, *32*, 2230−2231. (b) Craw, J. S.; Backsay, G. B.; Hush, N. S. *J. Am. Chem. Soc.* **1994**, *116*, 5937−5948.

for simplicity to analyze only one H−H couple, that highlighted in Figure 1, although an identical analysis could be carried out with all of them. Our B3LYP geometry optimization of **4b** within the $C_s$ symmetry gives very accurate results for the Os−$H_2$ fragment (Table 1), the discrepancy with experiment being inferior to 0.02 Å. Other parameters are also well reproduced by our calculation. The Os−$P_{axial}$ distances (experiment, 2.307, 2.317 Å; theory, 2.321, 2.323 Å) are properly found to be shorter than Os−$P_{equatorial}$ (experiment, 2.347; theory, 2.386 Å). Complex **4b** had also been previously subject of MP2 calculations, with results very similar to those presented here.[30]

In summary, we have presented in this section the results of the B3LYP geometry optimization for species **1b**−**4b** and shown that the results are in reasonable agreement with available data for complexes **1a**−**4a**. Moreover, we have shown that results with this method are at least of the same quality of previously published calculations with other methods on the same complexes. In the particular case of complex **2**, which seems to be the hardest to compute,[2,8] the results are clearly superior to MP2, which seems to be nowadays the main alternative. After showing that B3LYP provides a reasonable geometrical description of the systems, it can be expected that the electron density will also be well reproduced.

## Topological Analysis of Electron Density

The "atoms in molecules" (AIM) model of Bader and co-workers[10,11] provides one of the most powerful tools for the analysis of theoretical results. It can be applied to any computational method able to provide the electron density of the system. We are not aware of previous applications to DFT calculations on organometallic systems, but we attribute this to the relative scarceness of such calculations, since we cannot see any contradiction between the computational approach and the method of analysis.[33,34] The AIM scheme is based in the topological analysis of the electron density and its associated gradient and Laplacian. Here we are going to focus on a quite elementary analysis of the charge density function itself because this will suffice our purpose.

Although a complete explanation of the AIM methodology is beyond the scope of this paper, a brief comment belongs here. The properties of charge density, $\rho(\mathbf{r})$, which is a scalar property defined in all the 3-dimensional real space, are better characterized from a formal point of view in terms of its gradient vector field $\nabla\rho(\mathbf{r})$. The properties of this field, in turn, are totally determined by the number and character of its critical points, points at which the field vanishes. The trajectories of $\nabla\rho(\mathbf{r})$, all terminating at particular critical points, define the atoms in a molecule. Those which originate at the same critical points isolate the number, locations, and directions of lines throughout a charge distribution, linking particular pairs of atoms, along which the charge density is a maximum. This network of lines reproduces the essential features associated with the concept of bonding, and it is indeed postulated that

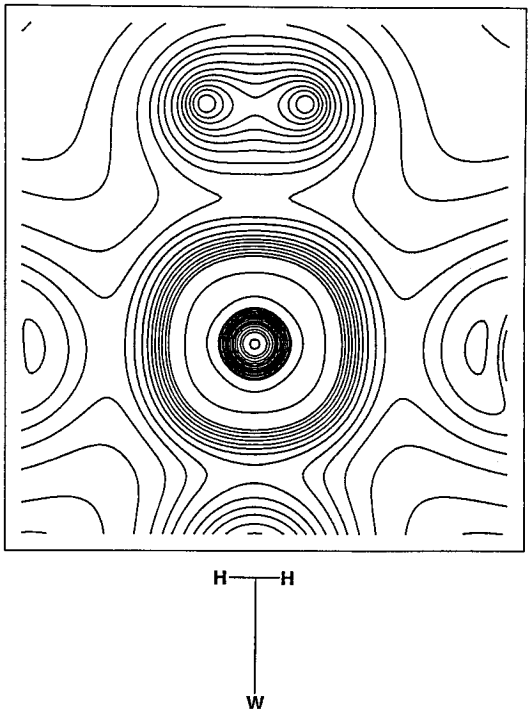


**Figure 2.** Electron isodensity contour map of the optimized system **1b**. The lines plotted correspond to the values of 0.0001, 0.001, 0.01, 0.02, 0.04, 0.06, 0.08, 0.10, 0.13, 0.16, 0.19, 0.22, 0.26, 0.30, 0.35, 0.40, 0.70, and 1.00 au.

these particular trajectories of $\nabla\rho(\mathbf{r})$, called bond paths, define the number, locations, and directions of chemical bonds in a molecule.[10,11] In summary, the basic idea is that atomic nuclei correspond to electron density maxima, and a bond path, characterized by a bond critical point, can be rigorously defined between each bound pair of atoms.

The AIM scheme appears therefore especially adequate for cases where chemical bonding between atoms cannot be clearly assigned from geometrical features and has indeed been applied before to dihydrogen species.[35,36] In both cases, which were positively identified as dihydrogen species, AIM gave a triangular bond structure, with the metal bound to each of the two hydrogen atoms and the hydrogen atoms linked to each other.

Figures 2−5 show the electron density plots corresponding to the B3LYP-optimized complexes **1b**−**4b**. All plots are done in the plane defined by the metal atom and the two hydrogens under study. The scale of the drawings is adjusted to show almost exclusively these three atoms. Although a larger scale would be more appropriate for a general view of the whole molecules, we have chosen this representation because it highlights the particular interaction between these three atoms. Some internal structure in the electron shells belonging to the metal can be noticed. It corresponds to the radial distribution of the metal valence electrons and can be observed only because the core electrons are absent from the drawing. An indicative bond structure is also presented in each of Figures 2−5, to indicate the

(33) Recently, a combined DFT/AIM analysis has been performed on a binuclear Rh(0) complex.[34]

(34) Bo, C.; Costas, M.; Poblet, J. M.; Rohmer, M.-M.; Bénard, M. *Inorg. Chem.*, in press.

(35) Maseras, F.; Duran, M.; Lledós, A.; Bertrán, J. *J. Am. Chem. Soc.* **1991**, *113*, 2879−2884.

(36) Dapprich, S.; Frenking, G. *Angew. Chem., Int. Ed. Engl.* **1995**, *34*, 354−357.

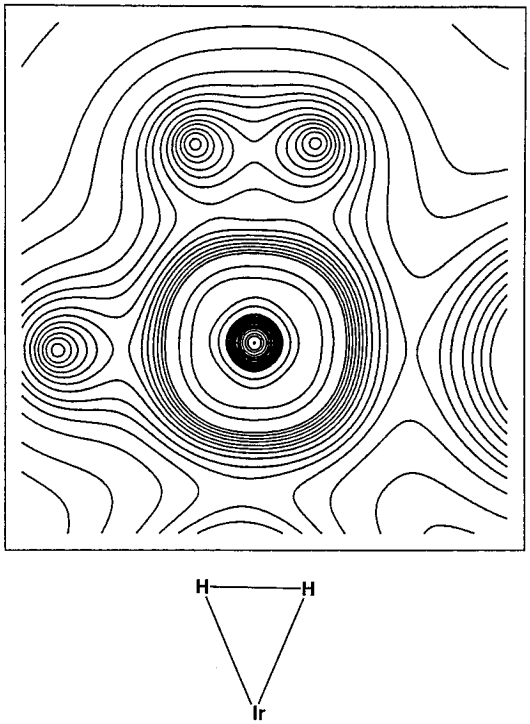


**Figure 3.** Electron isodensity contour map of the optimized system **2b**. The lines plotted correspond to the values of 0.0001, 0.001, 0.01, 0.02, 0.04, 0.06, 0.08, 0.10, 0.13, 0.16, 0.19, 0.22, 0.26, 0.30, 0.35, 0.40, 0.70, and 1.00 au.

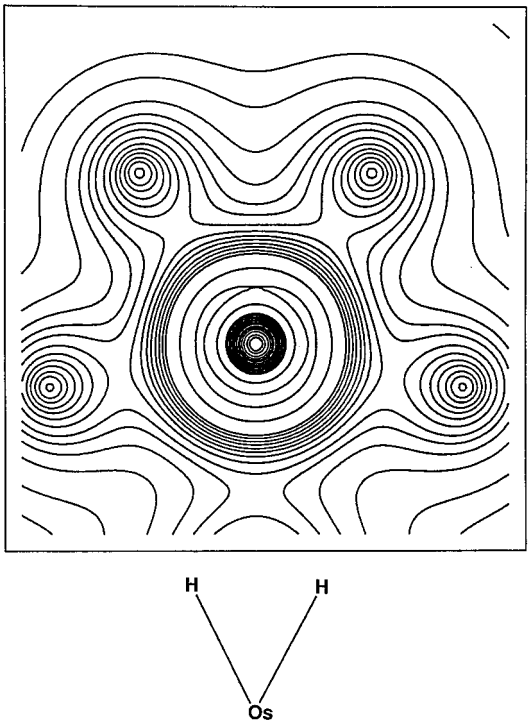


**Figure 5.** Electron isodensity contour map of the optimized system **4b**. The lines plotted correspond to the values of 0.0001, 0.001, 0.01, 0.02, 0.04, 0.06, 0.08, 0.10, 0.13, 0.16, 0.19, 0.22, 0.26, 0.30, 0.35, 0.40, 0.70, and 1.00 au.



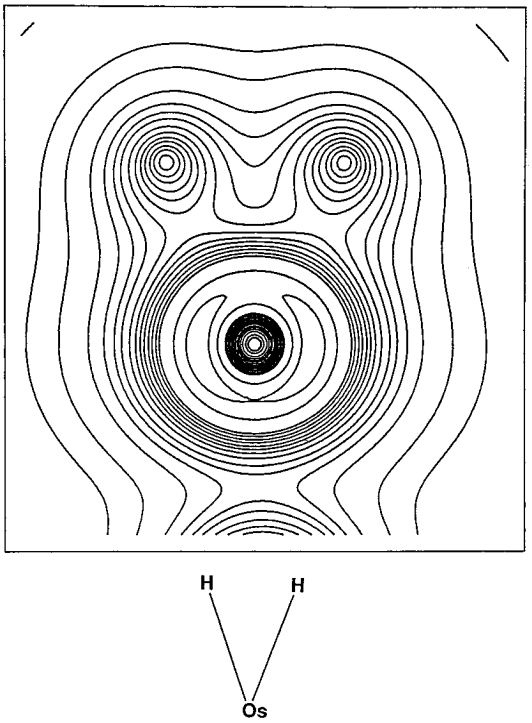


**Figure 4.** Electron isodensity contour map of the optimized system **3b**. The lines plotted correspond to the values of 0.0001, 0.001, 0.01, 0.02, 0.04, 0.06, 0.08, 0.10, 0.13, 0.16, 0.19, 0.22, 0.26, 0.30, 0.35, 0.40, 0.70, and 1.00 au.

interpretation the plots. Since this is one of the central points of this paper, we are going to analyze it in some detail how these bonding schemes can be inferred from the charge density distribution.

First, we begin by discussing complex **4b** (Figure 5), because **4a** is known from experiment to be a polyhydride complex, and this is formally the simplest structure to analyze with AIM. The large concentration of lines in the center of the plot corresponds to the metal atom. It is the clear maximum of electron density in this plot. Then, there are four other minor concentrations of density, two above the metal, one to its right, and another to its left. They correspond to the four hydrogen atoms directly attached to the metal, which are nearly coplanar in this pentagonal bipyramidal geometry. The phosphorus atom in this same plane would lie below the metal in the plot, should the picture be larger. We are going to focus on the two hydride ligands above the metal atom and the metal atom itself. As we have mentioned, the metal and the hydrogen atoms correspond to local maxima in the electron density. From a topological point of view, that means stationary points with three negative eigenvalues. In the region connecting each hydride to the metal there are also other stationary points. When going from the hydride to the metal, the density decreases, reaches a minimum in this direction, and then increases again. The point that is a minimum in this particular direction corresponds to a density maximum in the perpendicular direction within the picture, as can be seen. It would also correspond to a maximum in the third dimension, that perpendicular to the plane of the drawing. Therefore, this would be a stationary point (zero gradient), with one positive (minimum in one direction) and two negative (maximum in two directions) eigenvalues. This is the definition of bond critical point in the AIM theory. The lines connecting atomic nuclei with their corresponding bond critical points are the bond paths and define the bond chain of the molecule. This is precisely the meaning of the drawing in the bottom of Figure 5.

**Table 2. Bond Properties of the H−H and M−H Bonds in Complexes 1b−4b[a]**

| complex | bond | type | $\rho_b$ | $\nabla^2\rho_b$ | bond length[b] |
|---|---|---|---|---|---|
| **1b** | H−H | (3,−1) | 0.226 | −0.849 | 0.818 |
| | T−bond[c] | (3,−1) | 0.061 | +0.308 | |
| **2b** | H−H | (3,−1) | 0.164 | −0.296 | 0.984 |
| | Ir−H | (3,−1) | 0.127 | +0.266 | 1.651 |
| | | (3,+1) | 0.119 | +0.386 | |
| **3b** | Os−H | (3,−1) | 0.150 | +0.090 | 1.606 |
| **4b** | Os−H | (3,−1) | 0.138 | +0.075 | 1.641 |

[a] Atomic units: for $\rho$, 1 au = e/$a_0^3$ = 6.748 e Å$^{-3}$; for $\nabla^2\rho$, 1 au = e/$a_0^5$ = 24.10 e Å$^{-5}$. [b] In Å. [c] Bond critical point which links the maximum of charge density associated with the W atom and the H−H bond critical point.

A last remark concerning this figure will be especially relevant for the discussion that follows: there is no bond critical point connecting the two hydrogen atoms.

In Bader's formalism the properties of a bond are characterized by $\rho_b$ (density of the critical point) and $\nabla^2\rho_b$ (sum of the three curvatures of the Hessian matrix). Table 2 collects the bond properties obtained for the M−H and H−H bonds in complexes **1b**−**4b**. The values of $\rho_b$ and $\nabla^2\rho_b$ for the Os−H bond in complex **4b** are 0.138 and +0.075 au, respectively. It has been shown that positive values of Laplacian of charge density are characteristic of "closed-shell interactions". Ionic bonds are a typical case of such interactions. Studies on the coordinative bond with pure $\sigma$-donor or $\sigma$-donor and $\pi$-acceptor ligands also yielded positive values of $\nabla^2\rho_b$.[37] The relatively small value of the Laplacian of charge density at the bond critical point in **4b** suggests that this case is intermediate between closed-shell and shared interactions.

Let us discuss a second example of interpretation of density maps with the other complex having a well-known coordination mode. **1a** is positively characterized to be a dihydrogen complex. The density map of **4b** (Figure 5) is indeed sharply different from that of **1b** (Figure 2). In **1b** there is a very clear bond path connecting the two hydrogen atoms, in agreement with what should be expected from a dihydrogen complex. Another interesting feature is that the metal atom is not connected separately to each of the hydrogen atoms but rather directly to its bond critical point, giving therefore rise to a T-shaped bond structure, as drawn in the bottom of Figure 2. Thus, a (3,−1) critical point links a maximum of charge density with a bond path. A similar example has been reported for the minimum energy structure of the $CH_5^+$ ion. The topology of the charge density indicates that the structure of $CH_5^+$ corresponds to a $CH_3^+$ ion interacting with a hydrogen molecule.[38] The bond properties associated with the W−$H_2$ interaction and the H−H bond are also given in Table 2.

Finally, we should discuss Figures 3 and 4, representing complexes **2** and **3**, those whose coordination mode is under discussion. We feel that comparison of the four drawings is quite informative. Complex **2b** (Figure 3) presents a bond path between the two hydrogen atoms, characteristic of a dihydrogen complex (like **1b**, Figure 2). The values of $\nabla^2\rho_b$ for the H−H bond in **2b** are noticeably lower than those found in complex **1b** (see Table 2), as a consequence of the elongated nature of the dihydrogen bond. In contrast, in complex **3b** such a bond path is absent, as is the case for dihydride species (like **4b**, Figure 5). Therefore, on the basis of this analysis, we would say that **2a** is better described as dihydrogen than as dihydride complex, while **3a** is better described as a dihydride than as a dihydrogen complex. In other words, it seems appropriate to describe **2a** is an elongated dihydrogen complex, while **3a** would be better defined as a shortened dihydride complex. This difference is clearly perceptible on the maps of the Laplacian of $\rho$ computed for complexes **2b** and **3b** (Figure 6). The regions of charge concentration are represented by dotted lines in Figure 6. The distribution of $\nabla^2\rho_b$ in complex **2b** shows a region of charge concentration around the dihydrogen ligand. This distribution is quite similar to that of the $H_2$ molecule.[39] However, one can identify two separated charge concentrations associated with each of the hydride ligands in complex **3b**.

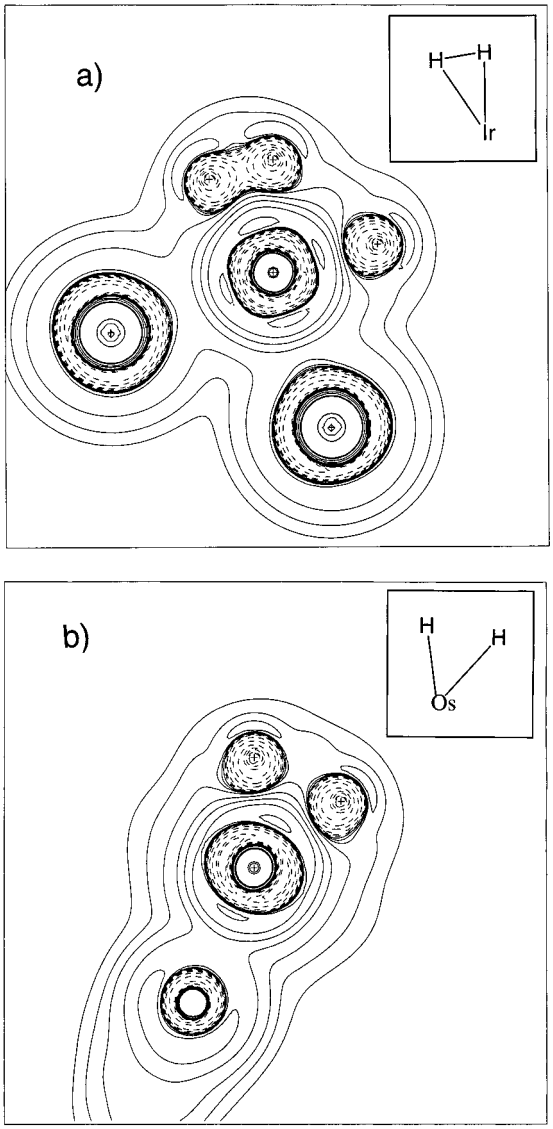


**Figure 6.** Plots of $\nabla^2\rho$ for complexes **2b** (a) and **3b** (b). Solid lines are for $\nabla^2\rho > 0$ (regions of charge depletion); dashed lines are for $\nabla^2\rho < 0$ (regions of charge concentration).

(37) (a) Bo, C.; Poblet, J. M.; Bénard, M. *Chem. Phys. Lett.* **1990**, *169*, 89−96. (b) Lin, Z.; Hall, M. B. *Inorg. Chem.* **1991**, *30*, 646−651. (c) Bo, C.; Sarasa, J. P.; Poblet, J. M. *J. Phys. Chem.* **1993**, *97*, 6362−6366.

(38) Reference 10, p 93.

(39) Reference 10, p 294.

**Table 3. Net Atomic Charges Computed for the Hydrogen Atoms from Integration of the Charge Density[a]**

| | 2b | 3b | 4b |
|---|---|---|---|
| $H_1$ | −0.008 | −0.177 | −0.212 |
| $H_2$ | −0.001 | −0.167 | −0.212 |

[a] The charge density integration of hydrogen atoms in complex **1b** has not been carried out (see text).

The last part of this section will be devoted to the analysis of the electronic population of the dihydrogen and hydride ligands. A realistic space partitioning has been proposed by Bader et al. and consists in defining the atomic domain as the three-dimensional basin limited by the surfaces of zero-gradient flux.[40] The electron population of an atom in a molecule is obtained by integration of $\rho(\mathbf{r})$ over the atomic domain. The computed net charges are given in Table 3. In agreement with the hydride nature of complexes **4b** and **3b**, the net charge of the hydride ligands is negative (−0.21 and −0.17 e, respectively). In contrast, the net charge close to zero computed for the $H_2$ unit in complex **2b** clearly indicates that there is a relationship between the electronic population of the hydrogen atoms and the H−H separation. Unfortunately, charge density integration in the $H_2$ unit of complex **1b** has not been possible because of the uncommon topology of the charge density distribution into the $W-H_2$ region. We find also of interest that the electronic population of the hydride ligand in the iridium complex **2b** (−0.15 e) is lower than the electronic population of hydride ligands in osmium complexes **3b** and **4b**. Moreover, the net charge for the other two hydride ligands in complex **4b** is −0.27 e. Therefore, Bader's net charges show that it is possible to relate the magnitude of metal to hydrogen charge transfer to the dihydrogen or dihydride nature of the complex.

(40) Bader, R. F. W.; Nguyen-Dang, T. T. *Adv. Quantum Chem.* **1981**, *14*, 63−124.

## Concluding Remarks

Theoretical analysis of the electron density of elongated dihydrogen [$ML_n(H\cdots H)$] complexes within the "atoms in molecules" scheme allows an unequivocal assignment of its nature. Certainly our study of $W(H_2)(CO)_3(PR_3)_2$, $IrH(H\cdots H)Cl_2(PR_3)_2$, $[Os(H\cdots H)(NH_2(CH_2)_2NH_2)_2(RCO_2)]^+$, and $OsH_4(PR_3)_3$ species shows the existence of two sharply different bonding patterns, one with an H−H bond and another without it. As expected, the structures of complexes $W(H_2)(CO)_3(PR_3)_2$ and $OsH_4(PR_3)_3$ respond to their known nature as dihydrogen and dihydride complexes, respectively. More significantly, the structure of species $IrH(H\cdots H)Cl_2(PR_3)_2$ and $[Os(H\cdots H)(NH_2(CH_2)_2NH_2)_2(RCO_2)]^+$, which lie in the twilight zone labeled as elongated dihydrogen complexes, can also be identified. According to this analysis, $IrH(H\cdots H)Cl_2(PR_3)_2$ would be a true elongated dihydrogen complex, while $[Os(H\cdots H)(NH_2(CH_2)_2NH_2)_2(RCO_2)]^+$ would be better labeled as a shortened dihydride complex.

More than the presentation of the results for these particular cases, the main goal of this work is to raise awareness on the great potential of the AIM method for the ellucidation of the nature of possible dihydrogen complexes, a field where other theoretical and experimental methods can be hardly applied. In this sense, we find the results presented here to provide an example of its success. In any case, we will welcome further discussion on the validity and limitations of the application of AIM to this particular problem of identification of the nature of dihydrogen complexes.

**Acknowledgment.** Financial support is acknowledged from the Spanish "Dirección General de Investigación Científica y Técnica" (DGICYT) under Project No. PB95-0639.

**Supporting Information Available:** Listings of the absolute energies and B3LYP-optimized Cartesian coordinates of complexes **1b**−**4b** (2 pages). Ordering information is given on any current masthead page.

OM950936U